Int. J. Mol. Sci. **2012**, *13*, 3782-3800; doi:10.3390/ijms13033782

OPEN ACCESS
International Journal of
Molecular Sciences
ISSN 1422-0067
www.mdpi.com/journal/ijms

Communication

Increasing the X-ray Diffraction Power of Protein Crystals by Dehydration: The Case of Bovine Serum Albumin and a Survey of Literature Data

Irene Russo Krauss [1], Filomena Sica [1,2], Carlo Andrea Mattia [3] and Antonello Merlino [1,2,*]

[1] Department of Chemical Sciences, University of Naples Federico II, Complesso Universitario di Monte Sant'Angelo, Via Cinthia, Naples I-80126, Italy; E-Mails: irene.russokrauss@unina.it (I.R.K.); filosica@unina.it (F.S.)
[2] Institute of Biostructures and Bioimages, CNR, Via Mezzocannone 16, Naples I-80134, Italy
[3] Department of Pharmaceutical and Biomedical Sciences, University of Salerno, Via Ponte Don Melillo, I-84084 Fisciano, Italy; E-Mail: mattia@unisa.it

***** Author to whom correspondence should be addressed; E-Mail: antonello.merlino@unina.it; Tel.: +39-081-674-276; Fax: +39-081-674-090.

Received: 9 February 2012; in revised form: 7 March 2012 / Accepted: 8 March 2012 / Published: 21 March 2012

Abstract: Serum albumin is one of the most widely studied proteins. It is the most abundant protein in plasma with a typical concentration of 5 g/100 mL and the principal transporter of fatty acids in plasma. While the crystal structures of human serum albumin (HSA) free and in complex with fatty acids, hemin, and local anesthetics have been characterized, no crystallographic models are available on bovine serum albumin (BSA), presumably because of the poor diffraction power of existing hexagonal BSA crystals. Here, the crystallization and diffraction data of a new BSA crystal form, obtained by the hanging drop method using MPEG 5K as precipitating agent, are presented. The crystals belong to space group *C*2, with unit-cell parameters a = 216.45 Å, b = 44.72 Å, c = 140.18 Å, β = 114.5 °. Dehydration was found to increase the diffraction limit of BSA crystals from ~8 Å to 3.2 Å, probably by improving the packing of protein molecules in the crystal lattice. These results, together with a survey of more than 60 successful cases of protein crystal dehydration, confirm that it can be a useful procedure to be used in initial screening as a method of improving the diffraction limits of existing crystals.

Keywords: serum albumin; protein crystallization; crystal dehydration; crystal quality; X-ray crystallography; post-crystallization treatment

1. Introduction

Serum albumins are the major soluble protein constituents of the circulatory system and have many physiological functions [1–3]. The most important property of this group of proteins is to serve as transporters for a variety of endogenous and exogenous compounds including metabolites, drugs and other biologically active substances, mostly through the formation of non-covalent complexes at specific binding sites [2]. Various investigations have studied the structure and properties of serum albumins and their interactions with small molecules or with other proteins [2,4,5]. Bovine serum albumin (BSA) is one of the most extensively studied of this group of proteins, particularly because of its structural homology with human serum albumin (HSA). BSA is also frequently used as a model system for physical chemistry studies, as it is an easily available, low cost, protein with unusual ligand-binding properties [5,6].

BSA is composed of a single chain of 583 amino acid residues including 35 cysteines (forming a total of 17 disulfide bridges), which confer a high stability to the protein. The molecular weight for BSA, calculated from different techniques, ranges from 66,411 to 66,700 Da and "the best value" in solution is 66,500 Da [1]. Its secondary structure is constituted by 67% α-helix and its isoelectric point (pI) is reported in a pH range of 4.8 to 5.6 [6–8]. The structure and properties of BSA in solution are characterized by a versatile conformation that is a function of pH, ionic strength, and the presence of ions [9].

The structure of BSA in aqueous solution has been extensively studied in the past by small-angle X-ray scattering [10], quasi-elastic light scattering [11], hydrodynamic techniques [12], neutron scattering [13] and ^{1}H NMR [14], but surprisingly its X-ray structure has not yet been solved. The main reason for this failure is that BSA crystals obtained up to now diffract to low resolution (the best diffraction obtained so far is 8 Å resolution) [15–17].

Here we describe the crystallization and preliminary X-ray diffraction studies of a new crystal form of BSA with two molecules in the asymmetric unit. We found that dehydration significantly improves the X-ray diffraction quality of these crystals. Dehydration is a post-crystallization treatment that tries to overcome the problems of loose packing of molecules and large solvent content, which are typical of protein crystals and lead to low-resolution diffraction. This procedure has previously been reported to increase the diffraction limit of many protein crystals. For a comprehensive survey of dehydration protocols the reader is referred to specific reviews which address this topic [18,19]. In this article, we also include a careful literature search of examples of improvements in X-ray diffraction properties of protein crystals, in an attempt to draw some conclusion from this review.

2. Results and Discussion

2.1. Crystallization of BSA

In the past, BSA crystals have been grown by a vapor diffusion technique from 50 mM potassium phosphate buffer, pH 6.2, 52% saturated ammonium sulphate at 298 K [15–17]. However, these crystals, which belong to space group P6 with unit cell parameters $a = b$ =148.24 Å, c = 356.70 Å and $\alpha = 90°$, $\beta = 90°$, $\gamma = 120°$, only diffract at low resolution (8–10 Å) [15,16].

Screening using polyethylene glycol of different molecular weights (2000–20,000 Da) as precipitating agent revealed new conditions for the crystallization of BSA. In particular, thin, small and fragile crystals appeared within 7 days using 30 mg mL^{-1} protein concentration with the hanging-drop method from crystallization conditions in which the reservoir solution contained 24% *w*/*v* MPEG 2K, 0.1 M Tris HCl pH 8. The quality of the crystals was improved by fine-tuning the concentration of protein (10.0–60.0 mg mL^{-1}), changing the precipitants and their concentration, and evaluating the effect of divalent cations, such as $CaCl_2$, $ZnCl_2$, $MgCl_2$. The best crystals (Figure 1a–e) were obtained from a crystallization solution containing 22–24% *w*/*v* MPEG 5K, 0.2M $MgCl_2$, 0.1 M Tris HCl pH 7.8, 8.0 and 8.2 and BSA at 20.0 mg mL^{-1}. Further optimizations of the crystallization conditions to grow larger and thicker crystals suitable for diffraction data collection at high resolution, using other methods (sitting drops or microbatch without oil [20]) failed.

Figure 1. Image of typical bovine serum albumin (BSA) crystals grown by vapour diffusion (**a**–**e**). Crystals obtained from a crystallization solution containing 22–24% *w/v* MPEG 5K, 0.2M $MgCl_2$, 0.1 M Tris HCl pH 7.8 (**a**–**c**) and 8 (**d**–**e**) and protein concentration of 20.0 mg mL^{-1}.

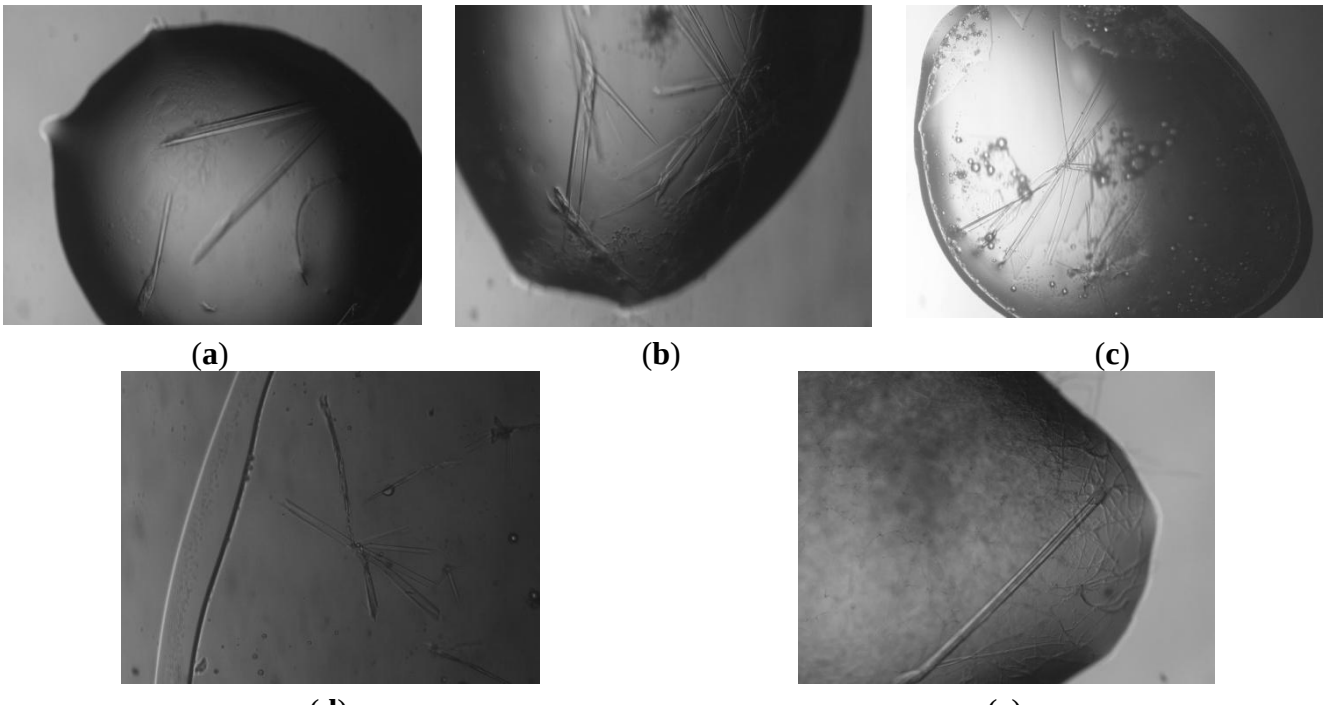

(**a**) (**b**) (**c**)

(**d**) (**e**)

Various cryosolutions (20% *v/v* glycerol, 300 mg mL^{-1} trehalose, 300 mg mL^{-1} saccharose) were prepared to examine their ability to cryoprotect the BSA crystals. Preliminary X-ray diffraction data collected at 100 K showed that even the best crystals (Figure 1a,b) were intrinsically disordered and that the largest ones diffracted at most to 8 Å resolution using glycerol as cryoprotectant. Application of an annealing protocol failed to improve the crystal diffraction quality. The latter method transiently returns the flash-cooled crystal to ambient temperature and has been shown to improve poor resolution and mosaicity, presumably caused by incorrect flash-cooling [21,22]. However, as reported in other cases [18,19,23–26], we found an increase in the diffraction power of BSA crystals by dehydration. A number of different trials for dehydrating crystals have been described in the literature. A comprehensive survey of the successfully used dehydration procedures is reported in Table 1 [18,19,24–85]. The dehydration process has been applied with success to crystals of proteins of various molecular weights, protein-protein and protein-ligand complexes. The resolution of the diffraction data collected from dehydrated crystals ranges from 1.1 Å to 4.5–5 Å, with resolution improvements that in some cases have been >10 Å; while the solvent content values range from 23% to 85%, with a decrease upon dehydration that generally has been <10%. The values of relative humidity in equilibrium with the solutions of the examined systems range from 74.3% to 99.5%. As expected, the best improvements in the X-ray diffraction power of protein crystals have been observed when the dehydration process has been applied to crystals with the highest solvent contents. Notably, the analysis of the Table suggests that even small changes in solvent content and relative humidity can promote favorable lattice rearrangements that dramatically improve the diffraction properties of crystals, as recently suggested by Russi *et al*. [26]. These findings underline the importance of reproducible and controlled crystal dehydration, such as that which can be obtained using modern devices available at synchrotron beamlines [86–88]. The data also confirm that at the start of a dehydration experiment, the relative humidity in equilibrium with the mother liquor is very often close to 100%, in agreement with recent data [89].

Table 1. Dehydration of protein crystals and effect on solvent content and diffraction resolution.

Protein crystal	Reference	Crystal precipitant[a]	Dehydrating agent	Dehydration treatment	Space group (SG)	Solvent content[b] before (%)	Solvent content[b] after (%)	RH before (%)	RH after (%)	Resolution before(Å)	Resolution after (Å)
BSA	This work	22% MPEG 5K	30% PEG 8K	Transfer to drop of dehydr soln, 10 min	C2	50-53	47	99.2	98.5	~8 [e]	3.2 [e]
DsbG	[24]	20% PEG 4K	30% PEG 4K	Transfer to drop of dehydr soln, hang over reservoir of dehydr soln,12h	C2	~90	53	99.3	98.4	~10[e]	2.0 [e] 1.7 [d]
FAD-indep ALS	[28]	6–8% PEG 8K 6–9% EG	Ppt 30% PEG 600	Hang over same dehydr soln, 12 h+ cryocool	C2	NR	52	NC	NC	2.9 [e]	2.6 [e]
Xis–DNA$^{X1\text{-}X2}$	[29]	30% PEG 4K	35–40% PEG 4K	Replacing both the well and hang-drop solutions with dehydr soln	$P3_121$ or $P3_221$	NR	59	98.4	96.9–97.7	10 [d]	2.6 [d]
Aldolase C	[30]	25% PEG 8K 4% glucose	25% PEG 8K 4% glucose	Replacing both the well and hang-drop solutions with dehydr soln	P1	NR	NR	NC	NC	NR	3.0 [e]
Aldolase B	[31]	1.8–2.2 M AS 2% diaminooctane	3.5 M AS	Replacing both the well and hang-drop solutions with dehydr soln	$P2_12_12$	NR	NR	91.2–93.0	85.3	NR	2.7 [e]
Tom20 receptor	[32]	15% PEG 6K	25% PEG 6K	Replacing both the well and hang-drop solutions with dehydr soln	C2	NR	NR	99.6	99.0	3–8 [d]	2.1 [d]
transamidosome	[33]	10% PEG 4K	30% PEG 400 10% PEG 4K	Replacing the reservoir solution with dehydr soln	$P2_12_12_1$ to $P2_1$ upon dehydr	NR	65	99.8	<97.1	4.0 [d]	3.0 [d]
X (or ADRP) domain of a variant of feline coronavirus	[34]	2.6–2.8 M AS	2.6–2.8 M AS 4-17% glycerol	Replacing the reservoir solution with dehydr soln 12h	$P4_12_12$	NR	78	NC	NC	4.5 [e]	3.1 [d]
SecDF	[35]	26% PEG 400	50% PEG 400	Replacing both the well and hanging-drop solutions with dehydr soln	$P4_32_12$	75	74	97.7	92.3	4.2 [d]	3.7 [d]
DsbC-DsbDα	[36]	25% MPEG 5K 5% glycerol	40% MPEG 5K 10% glycerol	Air dehydrate 30 min + cryocool	$P4_32_12$	55	41	NC	NC	7.0 [e]	3.8 [e] 2.3 [d]
Pyruvate Dehydrogenase	[37]	6% PEG 3K	Ppt 35% glycerol	Air dehydrate for 28 months, rehydrate in same soln, cryocool	R32	NR	73	99.9	90.5	7.0 [d]	4.2 [d]

Table 1. *Cont.*

Protein crystal	Reference	Crystal precipitant[a]	Dehydrating agent	Dehydration treatment	Space group (SG)	Solvent content[b] before (%)	Solvent content [b] after (%)	RH before (%)	RH after (%)	Resolution before(Å)	Resolution after (Å)
E. coli YbgL	[25]	0.8M sodium citrate	Ppt 10% EG	Annealing+air dehydrate (2 h)	C2	NR	57	NC	NC	~12[e]	2.6 [e] 1.8 [d]
E. coli YggV	[25]	35% AS	37.5% AS 10% glycerol	Annealing+air dehydrate (30 min)	$P4_32_12$	NR	38	89.5	<88.6	~12[e]	2.6 [e] 2.0 [d]
3-Dehydro dehy	[25]	11% PEG 8K	Ppt 10% glycerol	Annealing+air dehydrate (15 min)	$P2_1$	NR	88	99.8	<97.9	ND	3.0 [d]
Rv2002 gene product	[38]	20% PEG 3K	Ppt 10% MPD	Anneal + air dehydrate, 5 h	$P3_12\,1$	NR	35	NC	NC	2.1 [d]	1.8 [d]
Peptide deformylase	[39]	12% PEG 4K	20% PEG 4K 10% PEG 400	Anneal + air dehydrate, 30 min	$P2_12_12_1$	NR	50	99.7	<99.3	2.0 [d]	1.8 [d]
CLC Cl channel	[40]	22–32% Jeffamine	Ppt	Incub. in cryst. drop (5 months)	P222	NR	NR	NC	NC	7.5 [d]	4.0 [d]
Cytochrome ba_3 oxidase	[41]	14–16% PEG 2K	20% glycerol 20% EG	Incub. under oil 2–4 h/ air exp. 10 min	$P4_32_12$	NR	62	99.6-99.5	<93.2	4.0 [d]	2.3 [d]
5-Aminolaevulinic acid dehydratase	[42]	0.7 M 1,6-hexanediol		Air dehydrate, 30 min	$P\,4_22_12$	NR	41 or 61	NC	NC	NR	2.7 [d]
Pea chloroplast photosystem I	[26]	26% PEG 4K		Controlled relative humidity device	$P2_1$	NR	NR	99	97	6.0 [d]	4.0 [d]
Phosphoglycerate kinase	[26]	26% PEG 4K		Controlled relative humidity device	$P2_12_12$	NR	NR	98.5	97.5	3.0 [d]	1.8 [d]
Thioredoxin	[43]	10% PEG 1000		Controlled relative humidity device	$C222_1$	NR	NR	NR	NR	8.0 [d]	2.9 [d]
F1-ATPase	[44]	14% PEG 6K		Controlled relative humidity device	$P2_12_12_1$	NR	Reduction of 22%	99	90	NR	1.9 [d]
Dipeptidyl peptidase IV	[45]	20–22% PEG 2K		Controlled relative humidity device	P1	NR	NR	96.5	86.5	~10 [d]	3.0 [d]
Human GzmB	[46]	36% PEG 8K		Controlled relative humidity device	$P2_12_12_1$	NR	NR	90	85	NR	3.1 [d]
Tricorn Interacting Factor F3	[47]	18% PEG 2K		Controlled relative humidity device	$P3_221$	NR	NR	98	94	BD	2.3 [d]

Table 1. *Cont.*

Protein crystal	Reference	Crystal precipitant[a]	Dehydrating agent	Dehydration treatment	Space group (SG)	Solvent content [b] before (%)	Solvent content [b] after (%)	RH before (%)	RH after (%)	Resolution before(Å)	Resolution after (Å)
pMHC complexed with GTSGSPIADK	[48]	1.2 M K_2HPO_4 0.6 M NaH_2PO_4		Controlled relative humidity device	C2	NR	70	94.5	93.5	~7 [d]	3.2 [d]
RFC–PCNA	[50]	15% PEG 3.4K	33% PEG 3.4K	Serial transfer into increasing PEG 3.4K, 2h	$P2_12_12_1$	58	52	99.6	98.0	5.0 [d]	2.8 [d]
Penicillin G acylase	[51]	29% PEG 4K	36–70% PEG 4K 12–15% glycerol	Transfer to drop of dehydr soln (5–30 s)	$P2_1$	NR	46	98.5	<84.1	8.0 [e]	2.2 [e]
Cytochrome ba_3 oxidase mutants	[52]	6–7% PEG 2K	50% MPD, 14% PEG 2K	Transfer to drop of dehydr soln	$P4_32_12$ $P4_12_12$	NR	57–6	99.9	<99.6	2.6–3.0 [d]	2.3–2.4 [d]
ApoA-IV	[53]	22–28% PEG 3.4K	60% PEG 3.4K	Transfer to drop of dehydr soln,12h	P6	64	59	99.3–98.6	90.8	3.5 [d]	2.7 [d]
Plant photosystem I	[54]	0.5% PEG 400 3–5% PEG 6K	0.5% PEG 400 40% PEG 6K	Transfer to drop of dehydr soln, 1 week	$P2_1$	NR	NR	99.9	97.0	4.4 [d]	3.4 [d]
Nectin-1-EC complex	[55]	5% PEG 300	25% PEG 300	Transfer in var. steps to drop of dehydr soln	$P2_13$	NR	NR	99.6	97.4	~5 [d]	2.8 [d]
NgR	[56]	3.7 M NaCl	4.5 M NaCl	Transfer to drop of dehydr soln	$P3_121$	90	85	87.0	84.3	~5 [d]	3.2 [d]
Munc18c–syntaxin 41–29 complex	[57]	10–13% PEG 3.4K	25-30% PEG 3.4K	Transfer in var. steps to drop of dehydr soln	$P2_13$	54	53	99.8–99.7	98.9–98.4	4.3 [e]	3.7 [e]
HIV-RT:inhibitor	[58]	6% PEG 3.4K	46% PEG 3.4K	Serial transfer, 5% increments, 3 days	$P2_12_12_1$	56	48	99.9	95.5	3.7 [e]	2.2 [e]
Pp 1,2-CCD	[59]	14% PEG 8K	16–18% PEG 8K 20 % glycerol	Transfer to drop of dehydr soln, 30-60s	$P6_122$	NR	63	99.7	<95.3	8–10 [d]	~3.3 [d]
*ec*SecA	[60]	6–9% PEG 35K	2 M KCl	NR	$P2_1$	65	56	NC	NC	~3.5 [d]	2.0 [d]
MTCP-1	[61]	1.5 M AS	2.0 M AS	Soaked for 1–5 months	*P*6222	41	37	94.2	92.1	3.0 [e]	2.0 [e]
Trehalose phosphorylase	[27]	10% PEG 4K	18% PEG 4K	Various procedures	$P2_12_12_1$	NR	60	99.8	99.5	~7–8 [d]	~3–4 [d]
Glutaryl-7-aminocephalosporanic acid acylase	[62]	4% PEG 8K 10–20% PEG 4K	30% PEG 8K 20% glycerol	Transfer to drop of dehydr soln	$P2_12_12_1$	NR	NR	NC	NC	~4 [d]	1.6 [e]

Table 1. *Cont.*

Protein crystal	Reference	Crystal precipitant[a]	Dehydrating agent	Dehydration treatment	Space group (SG)	Solvent content[b] before (%)	Solvent content [b] after (%)	RH before (%)	RH after (%)	Resolution before(Å)	Resolution after (Å)
EIICGlc(1–412, K394A, M17T, K150E)	[63]	32–35% PEG 400	>80% PEG 400	Transfer to drop of dehydr soln, 48 h.	$P2_12_12_1$	NR	85	96.8–96.2	74.3	~8 [d]	4.5 [e]
MaoC-like dehydratase	[64]	5% PEG 6K	12% PEG 6K	Transfer to drop of dehydr soln, 30 min	$P2_12_12_1$	NR	NR	99.9	99.8	ND	1.9 [d]
Fatty acid synthase	[65]	4–5% PEG 6K	23% PEG 6K	Transfer to drop of dehydr soln,	$P2_12_12_1$ to $P2_1$ upon dehydr	67	65	99.9	99.2	~8 [d]	~5 [d]
Nur	[66]	5% PEG 6K, 5% MPD	15% PEG 6K, 10% MPD	Transfer to drop of dehydr soln, 20 min	$P3_1$	NR	65	99.9	<99.6	NR	2.4 [d]
Monoclinic lysozyme	[67]	10% NaCl	Satd NaCl solution	Transfer to drop of dehydr soln, 20 min	$P2_1$	29	23	91.1	79.3	1.4 [e]	1.1 [e]
His6-RepE–DNA1	[68]	10% PEG 4K	12% PEG 4K	Transfer to drop of dehydr soln, 36 h	$P2_1$	NR	63	99.8	99.8	~8 [d]	3.1 [d]
Ferredoxin reductase	[69]	16-18% PEG 10K	20% PEG 4K	Transfer to drop of dehydr soln, 15min	$P3_22_11$	NR	53	99.6–99.5	99.3	NR	2.2 [d]
MHC HLA-DQ2 complexed with gliadin peptides	[70]	25% PEG 4K	30% PEG 4K	dehydrated in a capillary containing dehydr soln, 3 days	I23	NR	40	98.9	98.4	~9 [d]	3.9 [e]
HCMV protease	[71]	16% PEG 4K	30% PEG 4K 0.15 M Na_2SO_4	Serial increase in reservoir conc, 3–5 days	$P4_12_12_1$	58	56	99.6	<98.4	3.0 [e]	2.5 [e] 2.0 [d]
Human STAT1	[72]	10–12% PEG 400	10.5% PEG 400 10–30% PEG 4K	Transfer in var. steps to drop of dehydr soln	$P6_122$	NR	60	NC	NC	3.7 [e]	3.0 [e]
Monoclinic lysozyme	[73]	3% $NaNO_3$	Satd K_2CrO_4 solution	Seal crystal in capillary, add plug of dehydr soln, for 15–20 h	$P2_1$	33	22	NC	NC	2.5 [e]	1.7 [e]
Tetragonal lysozyme	[74]	0.48–0.75 M NaCl	Satd salt solutions	Seal crystal in capillary, add plug of dehydr soln, for days to weeks	$P4_32_12$	NR	NR	98.3–97.3	79.3	3.7 [d]	1.6 [d]
MmeI in complex with DNA	[75]	10% PEG 8K	20% PEG 4K	Changing the mother liquor for crystal growth	P1	NR	NR	99.8	99.3	~4 [d]	2.6 [d]

Table 1. *Cont.*

Protein crystal	Reference	Crystal precipitant[a]	Dehydrating agent	Dehydration treatment	Space group (SG)	Solvent content[b] before (%)	Solvent content [b] after (%)	RH before (%)	RH after (%)	Resolution before(Å)	Resolution after (Å)
XRCC4–XLF complex	[76]	1.8 M TC	2.5 M AS	Transfer to 2.5 M AS 1 week + over 4 M AS, 5 days + 0.5 mM TB and 60% PEG 8000, 3 h	C2	NR	NR	NC	NC	~20 [d]	3.9 [d]
lipase–foldase complex	[77]	12% PEG 4K	30% PEG 8K	Transfer in var. steps to drop of dehydr soln	$P3_121$	62	60	99.8	98.5	~15 [d]	2.9 [d]
F1-ATPase	[78]	20% PEG 6K	20% PEG 6K 20% PEG 400	Serial transfer into dehydr soln	$P2_12_12_1$	NR	62	NC	NC	6–8 [d]	3.1 [d]
EF-Tu-Ts	[79]	20% PEG 4K	28%–40%, var PEGs	Serial transfer, 5 min each	$P2_12_12_1$	61	55	NC	NC	4.0 [e]	2.7 [e]
NF-κB P52-DNA	[80]	4–6% PEG 4K	Ppt 30% PEG 400 HA	Serial transfer into dehydr soln	$I2_12_12_1$	52	49	NC	NC	3.5 [d]	2.0 [d]
CBL1	[81]	25% PEG 3.4K	7% MPEG 2K 0.7 M Li_2SO_4	Transfer to dehydr soln, 5 min	$P2_12_12$	NR	54	NC	NC	NR	2.9 [d]
Cx26	[82]	16–18% PEG 200	25–30% TEG	Serial transfer into increasing TEG, 1-2days	C2	NR	NR	NC	NC	~7 [d]	3.5 [d]
Nacetylglucosamine -1-phosphate Uridyltransferase	[83]	1.8 M AS	2.0 M AS Na malonate 5% glycerol	Serial transfer into dehydr soln	I432	Very high solvent content	82	93.0	<92.1	3.8 [e]	3.4 [e]
SeMet YidC	[84]	22% PEG 3350 10% EG	30% PEG 3.4K 5–15% PEG 400	Serial transfer into dehydr soln	C2	50	47	NC	NC	3.5 [e]	1.8 [e]
DENV 3 RdRp	[85]	0.5% MPEG 5K	Var dehydr soln *i.e.*, 30% PEG 4K	Var procedures	$C222_1$	NR	59	NC	NC	~20 [d]	1.8 [d]

AS, ammonium sulphate, BD, bad diffraction; Dehydr soln, dehydrating solution; EG, ethylene glycol; hang drop, hanging drop; HA, heavy atom;MPD, 2-methyl-2,4-pentanediol; MPEG, PEG monomethylether; ND, no diffraction, NR, not reported; PEG, polyethylene glycol; ppt, precipitant; satd, saturated; TC, triammonium citrate, TB, tantalum bromide; TEG, triethylene glycol; var, various.

[a] Crystal precipitant information does not include details of buffers and other additives used in crystallization; [b] Solvent content was not always reported by authors. In some cases it has been calculated from information provided in the text of the paper; [c] Relative humidity (RH) values have been calculated using the online calculator available at http://go.esrf.eu/RH, as described by Bowler and co-workers [89]. Concentrations have been converted from *w/v* to *w/w* using: $w/w = w/v \text{ density}^{-1}$, where density values are taken from literature [90,91]; [d] X-ray diffraction resolution at a synchrotron source; [e] X-ray diffraction resolution on a rotating anode source.

Various dehydration protocols have been used. The dehydration process traditionally consists of equilibrating the protein crystals over a reservoir with a higher percentage of precipitant [24,28–35]. The hanging drop containing the crystals is then allowed to dehydrate for 12 h to 3 days. The simplest implementation involves dehydration by air [25,36–42]. Good results have been also obtained when protein crystals are mounted in a specific and adjustable stream of humidified gas, where it is possible to control the relative humidity [26,43–48,86–88]. Finally, crystal dehydration can also be performed by transferring the crystals into a dehydrating solution, which is the original mother liquor with a higher concentration of precipitant [24,27,50–70] or with a different dehydrating agent [49,71–85].

In the present case, common cryoprotectants, various salts (for example malonate) and different molecular-weight PEGs were tested as possible dehydration agents, but ultimately the most successful experiment was obtained when crystals which were grown in 22–24% *w/v* MPEG 5K, 0.2 M $MgCl_2$, 0.1 M Tris HCl pH 7.8 were directly transferred to a solution containing 30% *w/v* PEG 8K, 0.1M $MgCl_2$, 0.05 M Tris HCl pH 7.8. Crystals did not show any signs of cracking during dehydration. After dehydration and cryocooling, the diffraction resolution of the crystals on the in-house X-ray equipment improved to 3.24 Å resolution. The diffraction resolution could be even further improved with a synchrotron radiation source. Assuming the presence of two BSA molecules in the asymmetric unit, the crystal volume per unit molecular weight (V_M) is 2.3 $Å^3$ Da^{-1}, with a solvent content of 47%, which is within the normal range for protein crystals [92]. The solvent content of the crystals was reduced by 3-6% by dehydration. This process also produces a change in their relative humidity from 99.2% to 98.5%.

The application of molecular replacement, as detailed in the Experimental Section, enabled the identification of orientation and position of the two molecules in the asymmetric unit that gave a satisfactory fit to the experimental data. Refinement of the model, obtained by molecular replacement using phases derived from the structure of HSA is in progress.

The structural determination will provide a molecular basis for explaining numerous physical phenomena and for future docking and molecular dynamics studies on BSA complexes with drugs and other bioactive small molecules.

3. Experimental Section

3.1. Crystallization of BSA

Bovine serum albumin fraction V and all other reagents were purchased from Sigma Chemical Co. and used as supplied without further purification. BSA (80 mg/mL) was dissolved in 10 mM Tris-HCl buffer, pH 7.8. The protein concentration was determined spectrophotometrically using the extinction coefficient of 36,500 M^{-1} cm^{-1} at 280 nm [93].

Crystallization trials were performed at 293 K by the hanging-drop or sitting drop vapor-diffusion methods with 0.5 μL of protein and 0.5 μL of precipitant solution and a reservoir volume of 500 μL or using the microbatch without oil method [20] with the same volumes. Initial screens have included systematic PEG/pH and PEG/Ion screens. In particular, we prepared solutions with a formulation similar to the commercially available kits of Hampton Research. More than 100 different conditions were examined. In these crystallization experiments we varied the concentration of PEG from 10% *w/v*

to 30% *w/v*, the molecular weight of PEG from 2000 Da to 20,000 Da and the pH from 7 to 8. The effect of divalent cations, such as $CaCl_2$, $ZnCl_2$, $MgCl_2$ was also evaluated.

Needle crystals were obtained within 7 days from drops containing BSA (30 mg mL^{-1} in 10 mM Tris-HCl, pH 7.4) 24% *w/v* MPEG 2K and 0.1 M Tris HCl pH 8. An improvement in the quality of crystals was obtained using different salts and precipitant agents. In particular, well shaped crystals were grown using 22% *w/v* MPEG 5K, 0.2 M $MgCl_2$, 0.1 M Tris HCl pH 7.8 as a precipitant solution. These crystals diffracted to 8 Å resolution. In all the experiments, standard 24-well linbro plates (Hampton Research, Laguna Niguel, USA) were used.

3.2. Dehydration

A significant improvement in the crystal diffraction quality was obtained by dehydration with PEG 8K. In this procedure, protein crystals were transferred in a loop to a 5 μL solution containing 30% *w/v* PEG 8K, 0.05 M Tris HCl pH 7.8 and 0.1 M $MgCl_2$ for 10 min in the open air. After dehydration, the crystals were cryoprotected by soaking for 5–10 s in a solution consisting of 30% *w/v* PEG 8K, 0.05 M Tris HCl pH 7.8 and 0.1 M $MgCl_2$, 20% *v/v* glycerol and tested for diffraction quality as above.

3.3. Data collection and Processing

X-ray diffraction data (3.24 Å resolution) were collected at the Institute of Biostructures and Bioimages (Naples, Italy), at 100 K using a Rigaku MicroMax-007 HF generator producing Cu *Kα* radiation and equipped with a Saturn944 CCD detector. An oscillation range of 0.5 ° and an exposure time of 55 s were adopted for the experiments. The data sets were indexed, processed and scaled using the *HKL*-2000 package (Table 2) [94].

Table 2. Data collection statistics.

Space group	*C*2
Cell parameters	
a (Å)	216.45
b (Å)	44.72
c (Å)	140.18
β (°)	114.5
Resolution limits (Å)	50.00–3.24
Highest resolution shell (Å)	3.32–3.24
No. of observations	57717
No. of unique reflections	18006
Completeness (%)	88.8 (81.5)
I/*σ* (I)	5.5 (2.9)
Average multiplicity	3.2 (2.4)
R_{merge} (%)	15.4 (31.9)
Mosaicity	1.2

Note: Values in parentheses correspond to the highest resolution shell.

The overall R_{merge} was high at 15.4% and the R_{merge} value in the highest resolution bin was 31.9%. We attribute the high R_{merge} value as being primarily due to the large number of weak reflections that were measured and maybe to some radiation damage.

3.4. Structure Determination

The structure of the protein was solved by molecular replacement using the program Phaser [95] and HSA as search model (PDB code 2AO6 [96]). Water molecules were removed from the model prior to structure factor and phase calculations. The solution had an *R*-factor of 0.39.

4. Conclusions

For a long time the X-ray structure determination of BSA has been prevented due to the low diffraction power of its crystals. In this study, new BSA crystals were grown, X-ray diffraction data collected and the phase problem solved. BSA crystals that were initially unacceptable for structural analysis improved in diffraction limit by a process of dehydration. The best BSA crystals diffracted X-rays to a maximum resolution of 3.24 Å. Our results will be useful for numerous scientists who study the interactions of serum albumin with ligands, a field of interest for a great variety of biological, pharmaceutical, toxicological and cosmetic systems.

Our findings and previous literature results collected in Table 1 [18,19,24–85] confirm recent ideas that post-crystallization treatments can significantly improve X-ray diffraction protein crystal power. The analysis of the data does not enable us to define either a more promising dehydrating procedure or a more effective dehydrating agent. Rather, the review suggests that different procedures have to be tried, as the effects depend on both the protein nature and the crystal packing. Despite the high number of positive results, the technique remains little used. The take-home message of this work is that dehydration is one of the procedures that should be included in initial screening as a method to improve or at least modify the diffraction properties of existing crystals.

Acknowledgements

We acknowledge Giosu è Sorrentino and Maurizio Amendola (Institute of Biostructures and Bioimages, Naples, Italy) for technical assistance.

References

1. Carter, D.C.; Ho, J.X. Structure of serum albumin. *Adv. Protein Chem.* **1994**, *45*, 153–203.
2. Carter, D.C.; He, X.M.; Munson, S.H.; Twigg, P.D.; Gernert, K.M.; Broom, M.B.; Miller, T.Y. Three-dimensional structure of human serum albumin. *Science* **1989**, *244*, 1195–1198.
3. Figge, J.; Rossing, T.H.; Fencl, V. The role of serum proteins in acid-base equilibria. *J. Lab. Clin. Med.* **1991**, *117*, 453–467.
4. Sjoholm, I.; Ekman, B.; Kober, A.; Ljungstedt-Pahlman, I.; Seiving, B.; Sjodin, T. Binding of drugs to human serum albumin:XI. The specificity of three binding sites as studied with albumin immobilized in microparticles. *Mol. Pharmacol.* **1979**, *16*, 767–777.

5. He, X.M.; Carter, D.C. Atomic structure and chemistry of human serum albumin. *Nature* **1992**, *358*, 209–215.
6. Chakraborty, T.; Chakraborty, I.; Moulik, S.P.; Ghosh, S. Physicochemical and conformational studies on BSA-surfactant interaction in aqueous medium. *Langmuir* **2009**, *25*, 3062–3074.
7. Abou-Zied, O.K.; Al-Shihi, O.I. Characterization of subdomain IIA binding site of human serum albumin in its native, unfolded, and refolded states using small molecular probes. *J. Am. Chem. Soc.* **2008**, *130*, 10793–10801.
8. Sadler, P.J.; Tucker, A. pH-induced structural transitions of bovine serum albumin. Histidine pKa values and unfolding of the *N*-terminus during the N to F transition. *Eur. J. Biochem.* **1993**, *212*, 811–817.
9. Peters, T., Jr. Serum albumin. *Adv. Protein Chem.* **1985**, *37*, 161–245.
10. Riley, D.P.; Arndt, U.W. New type of x-ray evidence on the molecular structure of globular proteins. *Nature* **1952**, *169*, 138–139.
11. Doherty, P.; Benedek, G.B. The effect of electric charge on the diffusion of macromolecules. *J. Chem. Phys.* **1974**, *61*, 5426–5435.
12. Hughes, W.L. *The Proteins*; Neurath, H., Biley, K., Eds.; Academic Press: New York, NY, USA, 1954; Volume 2b, pp. 663–755.
13. Bendedouch, D.; Chen, S.H. Structure and interparticle interactions of bovine serum albumin in solution studied by small-angle neutron scattering. *J. Phys. Chem.* **1983**, *87*, 1473–1477.
14. Bos, O.J.; Labro, J.F.; Fischer, M.J.; Wilting, J.; Janssen, L.H. The molecular mechanism of the neutral-to-base transition of human serum albumin. Acid/base titration and proton nuclear magnetic resonance studies on a large peptic and a large tryptic fragment of albumin. *J. Biol. Chem.* **1989**, *264*, 953–959.
15. Thome, D.M. X-ray Crystallographic Studies of Thiomolybdates and Bovine Serum Albumin. Ph.D. thesis. Department of Chemistry, University of Saskatchewan, Saskatchewan, Canada, 2001.
16. Tai, H.C. X-ray Crystallographic Studies of Bovine Serum Albumin and Helicobacter Pylori Thioredoxin-2. Ph.D. Thesis, Department of Chemistry, University of Saskatchewan, Saskatchewan, Canada, 2004.
17. Asanov, A.N.; Delucas, L.J.; Oldham, P.B.; Wilson, W.W. Interfacial aggregation of bovine serum albumin related to crystallization conditions studied by total internal reflection fluorescence. *J. Colloid Interface Sci.* **1997**, *196*, 62–73.
18. Heras, B.; Martin, J.L. Post-crystallization treatments for improving diffraction quality of protein crystals. *Acta Crystallogr. D Biol. Crystallogr.* **2005**, *61*, 1173–1180.
19. Newman, J. A review of techniques for maximizing diffraction from a protein crystal in stilla. *Acta Crystallogr. D Biol. Crystallogr.* **2006**, *62*, 27–31.
20. Merlino, A.; Russo Krauss, I.; Albino, A.; Pica, A.; Vergara, A.; Masullo, M.; De Vendittis, E.; Sica, F. Improving protein crystal quality by the without-oil microbatch method: Crystallization and preliminary x-ray diffraction analysis of glutathione synthetase from pseudoalteromonas haloplanktis. *Int. J. Mol. Sci.* **2011**, *12*, 6312–6319.
21. Harp, J.M.; Timm, D.E.; Bunick, G.J. Macromolecular crystal annealing: Overcoming increased mosaicity associated with cryocrystallography. *Acta Crystallogr. D Biol. Crystallogr.* **1998**, *54*, 622–628.

22. Kriminski, S.; Caylor, C.L.; Nonato, M.C.; Finkelstein, K.D.; Thorne, R.E. Flash-cooling and annealing of protein crystals. *Acta Crystallogr. D Biol. Crystallogr.* **2002**, *58*, 459–471.
23. Cramer, P.; Bushnell, D.A.; Fu, J.; Gnatt, A.L.; Maier-Davis, B.; Thompson, N.E.; Burgess, R.R.; Edwards, A.M.; David, P.R.; Kornberg, R.D. Architecture of RNA polymerase II and implications for the transcription mechanism. *Science* **2000**, *288*, 640–649.
24. Heras, B.; Edeling, M.A.; Byriel, K.A.; Jones, A.; Raina, S.; Martin, J.L. Dehydration converts DsbG crystal diffraction from low to high resolution. *Structure* **2003**, *11*, 139–145.
25. Abergel, C. Spectacular improvement of X-ray diffraction through fast desiccation of protein crystals. *Acta Crystallogr. D Biol. Crystallogr.* **2004**, *60*, 1413–1416.
26. Russi, S.; Juers, D.H.; Sanchez-Weatherby, J.; Pellegrini, E.; Mossou, E.; Forsyth, V.T.; Huet, J.; Gobbo, A.; Felisaz, F.; Moya, R.; *et al*. Inducing phase changes in crystals of macromolecules: Status and perspectives for controlled crystal dehydration. *J. Struct. Biol.* **2011**, *175*, 236–243.
27. Van Hoorebeke, A.; Stout, J.; Van der Meeren, R.; Kyndt, J.; Van Beeumen, J.; Savvides, S.N. Crystallization and X-ray diffraction studies of inverting trehalose phosphorylase from Thermoanaerobacter sp. *Acta Crystallogr. Sect. F Struct. Biol. Cryst. Commun.* **2010**, *66*, 442–447.
28. Pang, S.S.; Guddat, L.W.; Duggleby, R.G. Crystallization of the FAD-independent acetolactate synthase of Klebsiella pneumoniae. *Acta Crystallogr. D Biol. Crystallogr.* **2002**, *58*, 1237–1239.
29. Sam, M.D.; Abbani, M.A.; Cascio, D.; Johnson, R.C.; Clubb, R.T. Crystallization, dehydration and preliminary X-ray analysis of excisionase (Xis) proteins cooperatively bound to DNA. *Acta Crystallogr. Sect. F Struct. Biol. Cryst. Commun.* **2006**, *62*, 825–828.
30. Arakaki, T.L.; Pezza, J.A.; Cronin, M.A.; Hopkins, C.E.; Zimmer, D.B.; Tolan, D.R.; Allen, K.N. Structure of human brain fructose 1,6-(*bis*)phosphate aldolase: linking isozyme structure with function. *Protein Sci.* **2004**, *13*, 3077–3084.
31. Malay, A.D.; Allen, K.N.; Tolan, D.R. Structure of the thermolabile mutant aldolase B, A149P: Molecular basis of hereditary fructose intolerance. *J. Mol. Biol.* **2005**, *347*, 135–144.
32. Igura, M.; Ose, T.; Obita, T.; Sato, C.; Maenaka, K.; Endo, T.; Kohda, D. Crystallization and preliminary X-ray analysis of mitochondrial presequence receptor Tom20 in complexes with a presequence from aldehyde dehydrogenase. *Acta Crystallogr. Sect. F Struct. Biol. Cryst. Commun.* **2005**, *61*, 514–517.
33. Bailly, M.; Blaise, M.; Lorber, B.; Thirup, S.; Kern, D. Isolation, crystallization and preliminary X-ray analysis of the transamidosome, a ribonucleoprotein involved in asparagine formation. *Acta Crystallogr. Sect. F Struct. Biol. Cryst. Commun.* **2009**, *65*, 577–581.
34. Wojdyla, J.A.; Manolaridis, I.; Snijder, E.J.; Gorbalenya, A.E.; Coutard, B.; Piotrowski, Y.; Hilgenfeld, R.; Tucker, P.A. Structure of the X (ADRP) domain of nsp3 from feline coronavirus. *Acta Crystallogr. D Biol. Crystallogr.* **2009**, *65*, 1292–1300.
35. Tsukazaki, T.; Mori, H.; Fukai, S.; Numata, T.; Perederina, A.; Adachi, H.; Matsumura, H.; Takano, K.; Murakami, S.; Inoue, T.; *et al*. Purification, crystallization and preliminary X-ray diffraction of SecDF, a translocon-associated membrane protein, from Thermus thermophilus. *Acta Crystallogr. Sect. F Struct. Biol. Cryst. Commun.* **2006**, *62*, 376–380.
36. Haebel, P.W.; Wichman, S.; Goldstone, D.; Metcalf, P. Crystallization and initial crystallographic analysis of the disulfide bond isomerase DsbC in complex with the alpha domain of the electron transporter DsbD. *J. Struct. Biol.* **2001**, *136*, 162–166.

37. Izard, T.; Sarfaty, S.; Westphal, A.; de Kok, A.; Hol, W.G. Improvement of diffraction quality upon rehydration of dehydrated icosahedral Enterococcus faecalis pyruvate dehydrogenase core crystals. *Protein Sci.* **1997**, *6*, 913–915.
38. Yang, J.K.; Yoon, H.J.; Ahn, H.J.; Lee, B.I.; Cho, S.H.; Waldo, G.S.; Park, M.S.; Suh, S.W. Crystallization and preliminary X-ray crystallographic analysis of the Rv2002 gene product from Mycobacterium tuberculosis, a beta-ketoacyl carrier protein reductase homologue. *Acta Crystallogr. D Biol. Crystallogr.* **2002**, *58*, 303–305.
39. Kim, H.W.; Han, B.W.; Yoon, H.J.; Yang, J.K.; Lee, B.I.; Lee, H.H.; Ahn, H.J.; Suh, S.W. Crystallization and preliminary X-ray crystallographic analysis of peptide deformylase from Pseudomonas aeruginosa. *Acta Crystallogr. D Biol. Crystallogr.* **2002**, *58*, 1874–1875.
40. Kuo, A.; Bowler, M.W.; Zimmer, J.; Antcliff, J.F.; Doyle, D.A. Increasing the diffraction limit and internal order of a membrane protein crystal by dehydration. *J. Struct. Biol.* **2003**, *141*, 97–102.
41. Hunsicker-Wang, L.M.; Pacoma, R.L.; Chen, Y.; Fee, J.A.; Stout, C.D. A novel cryoprotection scheme for enhancing the diffraction of crystals of recombinant cytochrome ba3 oxidase from Thermus thermophilus. *Acta Crystallogr. D Biol. Crystallogr.* **2005**, *61*, 340–343.
42. Lu, Q.; Ma, J.; Rong, H.; Fan, J.; Yuan, Y.; Li, K.; Gao, Y.; Zhang, X.; Teng, M.; Niu, L. Cloning, expression, purification, crystallization and preliminary crystallographic analysis of 5-aminolaevulinic acid dehydratase from Bacillus subtilis. *Acta Crystallogr. Sect. F Struct. Biol. Cryst. Commun.* **2010**, *66*, 1053–1055.
43. Koch, M.; Breithaupt, C.; Kiefersauer, R.; Freigang, J.; Huber, R.; Messerschmidt, A. Crystal structure of protoporphyrinogen IX oxidase: A key enzyme in haem and chlorophyll biosynthesis. *EMBO J.* **2004**, *23*, 1720–1728.
44. Bowler, M.W.; Montgomery, M.G.; Leslie, A.G.; Walker, J.E. Reproducible improvements in order and diffraction limit of crystals of bovine mitochondrial F(1)-ATPase by controlled dehydration. *Acta Crystallogr. D Biol. Crystallogr.* **2006**, *62*, 991–995.
45. Engel, M.; Hoffmann, T.; Wagner, L.; Wermann, M.; Heiser, U.; Kiefersauer, R.; Huber, R.; Bode, W.; Demuth, H.U.; Brandstetter, H. The crystal structure of dipeptidyl peptidase IV (CD26) reveals its functional regulation and enzymatic mechanism. *Proc. Natl. Acad. Sci. USA* **2003**, *100*, 5063–5068.
46. Estebanez-Perpina, E.; Fuentes-Prior, P.; Belorgey, D.; Braun, M.; Kiefersauer, R.; Maskos, K.; Huber, R.; Rubin, H.; Bode, W. Crystal structure of the caspase activator human granzyme B, a proteinase highly specific for an Asp-P1 residue. *Biol. Chem.* **2000**, *381*, 1203–1214.
47. Kyrieleis, O.J.; Goettig, P.; Kiefersauer, R.; Huber, R.; Brandstetter, H. Crystal structures of the tricorn interacting factor F3 from Thermoplasma acidophilum, a zinc aminopeptidase in three different conformations. *J. Mol. Biol.* **2005**, *349*, 787–800.
48. Chotiyarnwong, P.; Stewart-Jones, G.B.; Tarry, M.J.; Dejnirattisai, W.; Siebold, C.; Koch, M.; Stuart, D.I.; Harlos, K.; Malasit, P.; Screaton, G.; *et al*. Humidity control as a strategy for lattice optimization applied to crystals of HLA-A*1101 complexed with variant peptides from dengue virus. *Acta Crystallogr. Sect. F Struct. Biol. Cryst. Commun.* **2007**, *63*, 386–392.
49. Ke, A.; Doudna, J.A. Crystallization of RNA and RNA-protein complexes. *Methods* **2004**, *34*, 408–414.

50. Bowman, G.D.; O'Donnell, M.; Kuriyan, J. Structural analysis of a eukaryotic sliding DNA clamp-clamp loader complex. *Nature* **2004**, *429*, 724–730.
51. Rojviriya, C.; Pratumrat, T.; Saper, M.A.; Yuvaniyama, J. Improved X-ray diffraction from Bacillus megaterium penicillin G acylase crystals through long cryosoaking dehydration. *Acta Crystallogr. Sect. F Struct. Biol. Cryst. Commun.* **2011**, *67*, 1570–1574.
52. Liu, B.; Luna, V.M.; Chen, Y.; Stout, C.D.; Fee, J.A. An unexpected outcome of surface engineering an integral membrane protein: Improved crystallization of cytochrome ba(3) from Thermus thermophilus. *Acta Crystallogr. Sect. F Struct. Biol. Cryst. Commun.* **2007**, *63*, 1029–1034.
53. Deng, X.; Davidson, W.S.; Thompson, T.B. Improving the diffraction of apoA-IV crystals through extreme dehydration. *Acta Crystallogr. Sect. F Struct. Biol. Cryst. Commun.* **2012**, *68*, 105–110.
54. Amunts, A.; Drory, O.; Nelson, N. The structure of a plant photosystem I supercomplex at 3.4 A resolution. *Nature* **2007**, *447*, 58–63.
55. Narita, H.; Nakagawa, A.; Yamamoto, Y.; Sakisaka, T.; Takai, Y.; Suzuki, M. Refolding, crystallization and preliminary X-ray crystallographic study of the whole extracellular regions of nectins. *Acta Crystallogr. Sect. F Struct. Biol. Cryst. Commun.* **2011**, *67*, 344–348.
56. Barton, W.A.; Liu, B.P.; Tzvetkova, D.; Jeffrey, P.D.; Fournier, A.E.; Sah, D.; Cate, R.; Strittmatter, S.M.; Nikolov, D.B. Structure and axon outgrowth inhibitor binding of the Nogo-66 receptor and related proteins. *EMBO J.* **2003**, *22*, 3291–3302.
57. Latham, C.F.; Hu, S.H.; Gee, C.L.; Armishaw, C.J.; Alewood, P.F.; James, D.E.; Martin, J.L. Crystallization and preliminary X-ray diffraction of the Munc18c-syntaxin4 (1–29) complex. *Acta Crystallogr. Sect. F Struct. Biol. Cryst. Commun.* **2007**, *63*, 524–528.
58. Esnouf, R.M.; Ren, J.; Garman, E.F.; Somers, D.O.; Ross, C.K.; Jones, E.Y.; Stammers, D.K.; Stuart, D.I. Continuous and discontinuous changes in the unit cell of HIV-1 reverse transcriptase crystals on dehydration. *Acta Crystallogr. D Biol. Crystallogr.* **1998**, *54*, 938–953.
59. Rustiguel, J.K.; Pinheiro, M.P.; Araujo, A.P.; Nonato, M.C. Crystallization and preliminary X-ray diffraction analysis of recombinant chlorocatechol 1,2-dioxygenase from *Pseudomonas putida*. *Acta Crystallogr. Sect. F Struct. Biol. Cryst. Commun.* **2011**, *67*, 507–509.
60. Papanikolau, Y.; Papadovasilaki, M.; Ravelli, R.B.; McCarthy, A.A.; Cusack, S.; Economou, A.; Petratos, K. Structure of dimeric SecA, the Escherichia coli preprotein translocase motor. *J. Mol. Biol.* **2007**, *366*, 1545–1557.
61. Fu, Z.Q.; Du Bois, G.C.; Song, S.P.; Harrison, R.W.; Weber, I.T. Improving the diffraction quality of MTCP-1 crystals by post-crystallization soaking. *Acta Crystallogr. D Biol. Crystallogr.* **1999**, *55*, 5–7.
62. Anandan, A.; Vallet, C.; Coyle, T.; Moustafa, I.M.; Vrielink, A. Crystallization and preliminary diffraction analysis of an engineered cephalosporin acylase. *Acta Crystallogr. Sect. F Struct. Biol. Cryst. Commun.* **2010**, *66*, 808–810.
63. Zurbriggen, A.; Schneider, P.; Bahler, P.; Baumann, U.; Erni, B. Expression, purification, crystallization and preliminary X-ray analysis of the EIICGlc domain of the *Escherichia coli* glucose transporter. *Acta Crystallogr. Sect. F Struct. Biol. Cryst. Commun.* **2010**, *66*, 684–688.

64. Wang, H.; Guo, J.; Pang, H.; Zhang, X. Crystallization and preliminary X-ray analysis of the MaoC-like dehydratase from *Phytophthora capsici*. *Acta Crystallogr. Sect. F Struct. Biol. Cryst. Commun.* **2010**, *66*, 272–274.
65. Jenni, S.; Ban, N. Imperfect pseudo-merohedral twinning in crystals of fungal fatty acid synthase. *Acta Crystallogr. D Biol. Crystallogr.* **2009**, *65*, 101–111.
66. An, Y.J.; Ahn, B.E.; Roe, J.H.; Cha, S.S. Crystallization and preliminary X-ray crystallographic analyses of Nur, a nickel-responsive transcription regulator from *Streptomyces coelicolor*. *Acta Crystallogr. Sect. F Struct. Biol. Cryst. Commun.* **2008**, *64*, 130–132.
67. Harata, K.; Akiba, T. Effect of a sodium ion on the dehydration-induced phase transition of monoclinic lysozyme crystals. *Acta Crystallogr. D Biol. Crystallogr.* **2007**, *63*, 1016–1021.
68. Nakamura, A.; Wada, C.; Miki, K. Expression and purification of F-plasmid RepE and preliminary X-ray crystallographic study of its complex with operator DNA. *Acta Crystallogr. Sect. F Struct. Biol. Cryst. Commun.* **2007**, *63*, 346–349.
69. Peng, Y.; Xu, F.; Bell, S.G.; Wong, L.L.; Rao, Z. Crystallization and preliminary X-ray diffraction studies of a ferredoxin reductase from *Rhodopseudomonas palustris* CGA009. *Acta Crystallogr. Sect. F Struct. Biol. Cryst. Commun.* **2007**, *63*, 422–425.
70. Henderson, K.N.; Reid, H.H.; Borg, N.A.; Broughton, S.E.; Huyton, T.; Anderson, R.P.; McCluskey, J.; Rossjohn, J. The production and crystallization of the human leukocyte antigen class II molecules HLA-DQ2 and HLA-DQ8 complexed with deamidated gliadin peptides implicated in coeliac disease. *Acta Crystallogr. Sect. F Struct. Biol. Cryst. Commun.* **2007**, *63*, 1021–1025.
71. Tong, L.; Qian, C.; Davidson, W.; Massariol, M.J.; Bonneau, P.R.; Cordingley, M.G.; Lagace, L. Experiences from the structure determination of human cytomegalovirus protease. *Acta Crystallogr. D Biol. Crystallogr.* **1997**, *53*, 682–690.
72. Mao, X.; Chen, X. Crystallization and X-ray crystallographic analysis of human STAT1. *Acta Crystallogr. Sect. F Struct. Biol. Cryst. Commun.* **2005**, *61*, 666–668.
73. Madhusudan; Kodandapani, R.; Vijayan, M. Protein hydration and water structure: X-ray analysis of a closely packed protein crystal with very low solvent content. *Acta Crystallogr. D Biol. Crystallogr.* **1993**, *49*, 234–245.
74. Dobrianov, I.; Kriminski, S.; Caylor, C.L.; Lemay, S.G.; Kimmer, C.; Kisselev, A.; Finkelstein, K.D.; Thorne, R.E. Dynamic response of tetragonal lysozyme crystals to changes in relative humidity: Implications for post-growth crystal treatments. *Acta Crystallogr. D Biol. Crystallogr.* **2001**, *57*, 61–68.
75. Callahan, S.J.; Morgan, R.D.; Jain, R.; Townson, S.A.; Wilson, G.G.; Roberts, R.J.; Aggarwal, A.K. Crystallization and preliminary crystallographic analysis of the type IIL restriction enzyme MmeI in complex with DNA. *Acta Crystallogr. Sect. F Struct. Biol. Cryst. Commun.* **2011**, *67*, 1262–1265.
76. Andres, S.N.; Junop, M.S. Crystallization and preliminary X-ray diffraction analysis of the human XRCC4-XLF complex. *Acta Crystallogr. Sect. F Struct. Biol. Cryst. Commun.* **2011**, *67*, 1399–1402.
77. Pauwels, K.; Loris, R.; Vandenbussche, G.; Ruysschaert, J.M.; Wyns, L.; Van Gelder, P. Crystallization and crystal manipulation of a steric chaperone in complex with its lipase substrate. *Acta Crystallogr. Sect. F Struct. Biol. Cryst. Commun.* **2005**, *61*, 791–795.

78. Stocker, A.; Keis, S.; Cook, G.M.; Dimroth, P. Purification, crystallization, and properties of F1-ATPase complexes from the *thermoalkaliphilic Bacillus* sp. strain TA2.A1. *J. Struct. Biol.* **2005**, *152*, 140–145.
79. Schick, B.; Jurnak, F. Crystal growth and crystal improvement strategies. *Acta Crystallogr. F* **1994**, *50*, 563–568.
80. Cramer, P.; Muller, C.W. Engineering of diffraction-quality crystals of the NF-kappaB P52 homodimer:DNA complex. *FEBS Lett.* **1997**, *405*, 373–377.
81. Shang, G.; Cang, H.; Liu, Z.; Gao, W.; Bi, R. Crystallization and preliminary crystallographic analysis of a calcineurin B-like protein 1 (CBL1) mutant from *Ammopiptanthus mongolicus*. *Acta Crystallogr. Sect. F Struct. Biol. Cryst. Commun.* **2010**, *66*, 1602–1605.
82. Suga, M.; Maeda, S.; Nakagawa, S.; Yamashita, E.; Tsukihara, T. A description of the structural determination procedures of a gap junction channel at 3.5 A resolution. *Acta Crystallogr. D Biol. Crystallogr.* **2009**, *65*, 758–766.
83. Verma, S.K.; Jaiswal, M.; Kumar, N.; Parikh, A.; Nandicoori, V.K.; Prakash, B. Structure of *N*-acetylglucosamine-1-phosphate uridyltransferase (GlmU) from *Mycobacterium tuberculosis* in a cubic space group. *Acta Crystallogr. Sect. F Struct. Biol. Cryst. Commun.* **2009**, *65*, 435–439.
84. Ravaud, S.; Wild, K.; Sinning, I. Purification, crystallization and preliminary structural characterization of the periplasmic domain P1 of the *Escherichia coli* membrane-protein insertase YidC. *Acta Crystallogr. Sect. F Struct. Biol. Cryst. Commun.* **2008**, *64*, 144–148.
85. Yap, T.L.; Chen, Y.L.; Xu, T.; Wen, D.; Vasudevan, S.G.; Lescar, J. A multi-step strategy to obtain crystals of the dengue virus RNA-dependent RNA polymerase that diffract to high resolution. *Acta Crystallogr. Sect. F Struct. Biol. Cryst. Commun.* **2007**, *63*, 78–83.
86. Kiefersauer, R.; Than, M.E.; Dobbek, H.; Gremer, L.; Melero, M.; Strobl, S.; Dias, J.M.; Soulimane, T.; Huber, R. A novel free-mounting system for protein crystals: transformation and improvement of diffraction power by accurately controlled humidity changes. *J. Appl. Cryst.* **2000**, *33*, 1223–1230.
87. Sanchez-Weatherby, J.; Bowler, M.W.; Huet, J.; Gobbo, A.; Felisaz, F.; Lavault, B.; Moya, R.; Kadlec, J.; Ravelli, R.B.; Cipriani, F. Improving diffraction by humidity control: A novel device compatible with X-ray beamlines. *Acta Crystallogr. D Biol. Crystallogr.* **2009**, *65*, 1237–1246.
88. Sjogren, T.; Carlsson, G.; Larsson, G.; Hajdu, A.; Andersson, C.; Pettersson, H.; Hajdu, J. Protein crystallography in a vapour stream: Data collection, reaction initiation and intermediate trapping in naked hydrated protein crystals. *J. Appl. Cryst.* **2002**, *35*, 113–116.
89. Wheeler, M.J.; Russi, S.; Bowler, M.G.; Bowler, M.W. Measurement of the equilibrium relative humidity for common precipitant concentrations: Facilitating controlled dehydration experiments. *Acta Crystallogr. Sect. F Struct. Biol. Cryst. Commun.* **2012**, *68*, 111–114.
90. Eliassi, A.; Modarress, H. Densities of poly(ethylene glycol) + water mixtures in the 298.15-328.15 K temperature range. *J. Chem. Eng. Data* **1998**, *43*, 719–772.
91. Alcorn, T.; Juers, D.H. Progress in rational methods of cryoprotection in macromolecular crystallography. *Acta Crystallogr. D Biol. Crystallogr.* **2010**, *66*, 366–373.
92. Matthews, B.W. Solvent content of protein crystals. *J. Mol. Biol.* **1968**, *33*, 491–497.
93. Painter, L.; Harding, M.M.; Beeby, P.J. Synthesis and interaction with human serum albumin of the first 3,18-disubstituted derivative of bilirubin. *J. Chem. Soc. Perkin Trans.* **1998**, *18*, 3041–3050.

94. Otwinowsky, Z.; Minor, W. Processing of X-ray diffraction data collected in oscillation mode. *Methods Enzymol.* **1997**, *276*, 307–326.
95. Storoni, L.C.; McCoy, A.J.; Read, R.J. Likelihood-enhanced fast rotation functions. *Acta Crystallogr. D Biol. Crystallogr.* **2004**, *60*, 432–438.
96. Sugio, S.; Kashima, A.; Mochizuki, S.; Noda, M.; Kobayashi, K. Crystal structure of human serum albumin at 2.5 A resolution. *Protein Eng.* **1999**, *12*, 439–446.